Identification and Analysis of Reverse-Bias Breakdown Sites in CIGS Solar Cells from Modules to Atoms

Jun Liu, Steve Johnston, Harvey Guthrey, and Mowafak Al-Jassim

National Renewable Energy Laboratory, Golden, Colorado, 80401, U.S.A.

Copper indium gallium diselenide (CIGS)-based solar cell is a promising and cost-saving alternative to silicon-based solar cell, with a demonstrated efficiency of 22.6% [1]. However, partial shading can initiate reverse-bias breakdown in CIGS modules, resulting in permanent wormlike defects due to thermal runaway. This leads to permanent power losses (open circuit voltage and fill factor) for the modules. Bypass diodes are mounted on the modules to disable operation under reverse-bias condition, however, a significant portion of the module can be shaded (up to 20%) before the diodes are activated. A better understanding of where and how the breakdown occurs is necessary to tailor the manufacturing process to improve the reliability and reduce the cost of modules.

Dark lock-in thermography (DLIT) under reverse-bias with a current limit is used to quickly acquire a thermal image of a module and locate the hot-spot heating sites where breakdown likely occurs before a thermal runaway event is initialed. A coring technique has been developed to cut the hot-spot heating sites from the module using a diamond-based coring bit and drill [2]. The breakdown sites, normally within the solar cells absorbers, can be accurately located via scanning electron microscopy (SEM) coupled with electron beam induced current (EBIC). Once identified, transmission electron microscopy (TEM) foils are prepared by standard lift-out technique using focusing ion beam (FIB) with a Pt capping layer to protect the surface of breakdown sites. The structure and chemistry of the breakdown sites can be studied at atomic-scale using TEM.

Figs. 1 (a)-(b) are reverse-bias DLIT images using a sufficiently-high voltage for breakdown with a current limit of ~0.3 mA/cm^2. DLIT images exhibit six hot-spot heating sites in the module. One heating site (S1) locates within the field of cells (named as cell defect), while the other five are near or on the scribe lines. Among them, two heating sites (S2 and S3) are on P3 scribe line (named as P3 defect), and the other three (S4, S5, and S6) occur on P1 scribe line (named as P1 defect). The DLIT images suggest the reverse-bias breakdown can occur at any weak sites of the module but have preference to propagate along scribe lines [3-5]. Fig. 1 (c) is the plane-view SEM image from the cell defect S1 in Fig. 1 (a) and the surface is flat in this case, although breakdown sites normally exhibit nodule or crater features a few micrometers in size. The EBIC image in Fig. 1 (d) taken from the same region as Fig. 1 (c) shows a dark-contrast circle with diameter of 40 µm, indicating the existence of buried defects causing a reduction in the collected current through the enhanced recombination of electrons and holes at this location. FIB milling is used to view the buried defects in cross section as shown in Fig. 1 (e) and the SEM image clearly reveals the buried defects in the form of voids or pinholes in the thin film.

Fig. 2 is a scanning transmission electron microscopy-high angle annular dark field (STEM-HAADF) image and corresponding STEM-energy-dispersive X-ray spectroscopy (STEM-EDS) elemental mappings of cell defect S1. The STEM-HAADF image in Fig. 2 (a) shows two large voids with ~2 µm and several small voids in a few hundred nanometers. In addition, there is a contrast variation in CIGS layer, which indicates nonuniform absorber chemistry at the breakdown sites. The voids are mostly located at the top of the CIGS layer, as shown in Figs. 2 (b)-(h). The Zn appears to diffuse into the CIGS

layer, and there is no clear interface between ZnO and CIGS in this region. Cu rich and Cu/In rich particles are seen in the CIGS layer. A separation of Ga and Se can be found in Figs. 2 (g)-(h). In summary, the CIGS layer at the cell defect identified by the DLIT image is totally decomposed and dispersed with voids.

The same analysis approach is performed on P1 defect and P3 defect. For P1 defect, without Mo layer, a large porous nodule is often found in CIGS layer. For P3 defect, there is a damaged CIGS layer, but no ZnO layer. In both cases, Ga content has been drastically reduced in CIGS layer.

In this work, multi-scale characterization techniques including DLIT, SEM, EBIC, and TEM were applied to a CIGS module to locate and analyze different types of reverse-bias breakdown sites. The decomposed CIGS layer is detrimental to module performance and provides insight into the origins of the formation of wormlike defects under partial shading.

References:
[1] M Powalla *et al*, Engineering **3** (2017), p. 445.
[2] S Johnston *et al*, Proceeding of the 43rd IEEE Photovoltaic Specialist Conference (2016), p. 0889.
[3] EE van Dyk, C Radue, and AR Gxasheka, Thin Solid Films **515** (2007), p. 6196.
[4] P-O Westin *et al*, the 24th European Photovoltaic Solar Energy Conference (2009).
[5] JE Lee *et al*, Progress in Photovoltaics: Research and Applications **24** (2016), p. 1035.

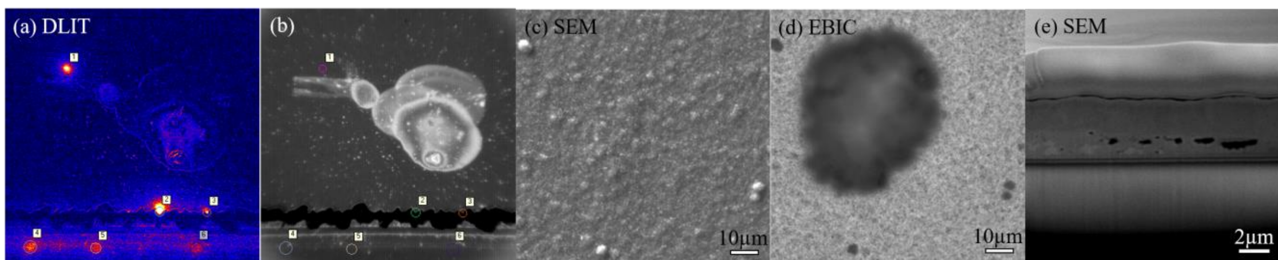

Figure 1. (a)-(b) reverse-bias DLIT images. (c) plane-view SEM image from cell defect S1 in Fig. 1 (a). (d) EBIC image taken from the same region as Fig. 1 (c). (e) cross-sectional SEM image of cell defect S1.

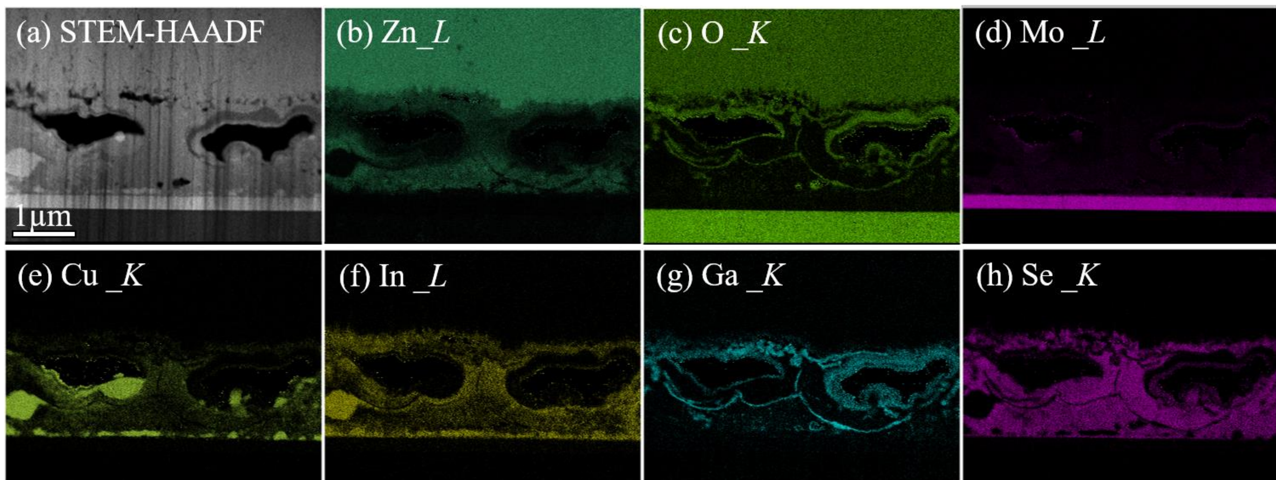

Figure 2. (a) STEM-HAADF image of cell defect S1. Elemental mappings of cell defect S1, (b) Zn_*L*, (c) O_*K*, (d) Mo_*L*, (e) Cu_*K*, (f) In_*L*, (g) Ga_*K*, (h) Se_*K*.